METEOROLOGY OF THE SOUTHERN GLOBAL PLUME: AFRICAN AND SOUTH AMERICAN FIRES POLLUTE THE SOUTH PACIFIC

Z. GUO+*, R. B. CHATFIELD*
+San Jose State University, San Jose CA
*NASA Ames Research Center, Moffett Field CA

Abstract — An immense global plume of CO meanders widely around the world in the Southern Hemisphere. It arises over Southern America and Africa and flows eastward. The first emissions are in tropical Brazil, and the plume circulates around the world to South America again. The plume was largely unexpected until there were aircraft studies made in NASA's Pacific Exploratory Mission - Tropics (Part A). This paper describes the meteorology of the Global Plume, as our simulation, with a synoptic model adapted to global transport, reveals it with a tracer-CO simulation. The observations and their simulation require a particular set of conditions of pollutant accumulation, cumulonimbus venting with required strengths at a narrow range of altitude. Additionally, a particular subtropical conduction region, over the Indian Ocean, Australia, and the westernmost South Pacific, relatively free of storms, appears to be a key part of the mechanism. These conclusions are the results of a synoptic reconstruction of the PEMT-A period, September-October, 1996.

INTRODUCTION

When the Pacific Exploratory Mission Tropics (Part A) - PEMT-A - was planned, it mainly appeared an opportunity to sample the clean atmosphere. Although pollution was known to occur in the Southern Hemisphere, it was presumed to be concentrated mainly in the South Tropical Atlantic and its adjoining continents. There was considerable surprise when the DC-8 aircraft repeatedly discovered plumes of pollution, evidently mostly from biomass burning. For the plumes sampled in the South Pacific, questions immediately arose (i) How typical was the sampling along the chosen DC-8 flight paths? (ii) To what extent were the plumes a feature of just one exotic month during the year, or to what extent did they describe a broader seasonal pattern? Most importantly, of course, came the question: (iii) if these were signals of biomass burning pollution, where did they come from and how did they get to the mid-Pacific? To the extent that the plumes did modify a significant amount of the Pacific large-scale chemistry, there is a fourth question: (iv) what algorithms, parameterizations, and what numerical parameter settings are necessary to represent this global pollution chemistry?

METHODS

MM5 Simulations

The fifth-generation PSU/NCAR mesoscale model (MM5) was used to provide hourly weather conditions for this study. MM5 is a three-dimensional, primitive-equation model with terrain-following sigma coordinates (Grell et al., 1995). The model simulation domain has 37x160 grid points and 23 sigma levels. The nominal grid size is 249 KM and the top layer is 70 hPa. The initial and lateral boundary conditions were interpolated from 2.5 x 2.5 global objective analyses supplied by European Centre for Medium-Range Weather Forecasts (ECMWF). These analyzed fields are also used for four-dimensional data assimilation (FDDA). An analysis-nudging FDDA approach is applied continuously to force the model simulated wind components (u,v), temperature (T) and water vapor mixing ratio (qv) toward grided analyses based on the observations.

The convective parameterization suggested by Grell (Grell, 1993, Grell et al, 1995) is used for the non-resolved convective motion. The information on hourly averaged cloud tops, cloud bases, heights of downdraft levels, strength of downdraft and mass fluxes of clouds is output to a history file.

The GRACES Model

We employed our GRACES (Global Regional Atmospheric Chemistry Event Simulator) model much as described previously in Chatfield et al. (1996) and Chatfield et al. (1998). The record of winds, temperatures, surface pressures, boundary-layer mixing heights, and Grell-scheme parameters from the MM5 history was used to drive the model. GRACES runs on essentially the same grid as MM5; Arakawa B-grid winds from MM5 are simply averaged for use on GRACES Arakawa C-Grid (Arakawa and Lamb, 1977). Cloud fluxes of carbon monoxide are extremely important in explaining CO distributions (Pratt and Falconer, 1979 , Dickerson et al., 1987, Chatfield and Delany, 1990) and correct mass-transport paramaterizations are essential to estimates of the CO budget (Chatfield et al., 1998). Subgrid vertical transport of CO in cumulonimbus clouds is

parameterized by using a single upward pipe and a single downward pipe; that is, entrainment of air in core updrafts and downdrafts is ignored (Grell et al., 1995). Our previous experience with the TRACE-A data suggested that this disregard of entrainment, or other causes, may have underestimated vertical transport, although locations of convection appeared to be acceptably forecast. Following Chatfield et al. (1998), then, we multiply the vertical transports in the pipes by a factor of 2.5, and set other (environmental-air) transports to conserve mass. Additionally, we spread the detrainment of material at cloud top over the top three layers, with one half at the cloud-top the Grell scheme provides, one-third in the layer below, and the rest in the next layer down.

Carbon monoxide is treated as a passive tracer without chemical loss or production in the atmosphere. CO is produced by methane in the free atmosphere to a compensation level of somewhere below 40 ppb, and even more is produced within a biomass burning plume with increased levels of methane and other organics. The behavior of our CO tracer in this simulation is therefore of an accumulating tracer whose concentrations are kept bounded by the 50-ppb northern and southern boundary conditions; the boundary conditions and the length of simulation tend to set a reasonable level of non-plume CO

RESULTS AND DISCUSSION

Statistical Comparisons of Observations and Simulation

Figure 1 shows comparisons of the CO observed during the DC-8 flights made in the South Pacific and our simulation of the biomass-burning CO tracer. Histograms present the number of incidences of CO in each of four different layers of the atmosphere. The left column shows the histogram of observed CO along the aircraft flight tracks, as measured by the Sachse NASA Langley group. The right column shows samples from the model along the same flight tracks and the same times, figuratively "flying the plane through the model
results."

Table 1 gives the median, mean and standard deviation of Observed and simulated CO.

Table 1. Mean and Standard Deviation for Observed and model CO

	OBS	MODEL	
median	55.9300	61.8800	
mean	58.7150	62.4520	--> 200-400 hPa
Sdev	11.1260	4.19691	
median	60.3100	62.1500	
mean	69.5730	62.4452	--> 400-600 hPa
Sdev	25.6856	4.00454	
median	60.6700	59.3000	
mean	63.2366	58.8764	--> 600-800 hPa
Sdev	11.1307	5.51434	
median	53.5000	57.8500	
mean	56.4003	57.8709	--> 800-1000 hPa
Sdev	7.27314	4.97084	

It may be seen from the graphic and the table that the DC-8 may have made a reasonably representative sampling of the Equatorial and South Pacific. The mean status of CO are simulated very well. On average, the model CO is a little bit larger than observed CO on upper and lower atmosphere. The larger standard deviation shows the observations having of some relatively smaller scale feature. The model obviously underestimates CO extremes.

Study of a Mid-Tropospheric Plume: Sept. 14, 1996

Trajectory analysis of the origins of the plume. Figure 2(g) shows a map view of the plume obtained from our GRACES run. A wispy trace of the plume can be seen around the 180 line, especially just to the west of the line. The origins of the plume at our kilometers can be traced back by the MM5 trajectory and tracer analyses. That is, In a air-composition-origin techniques, concentration maxima, indicating plumes, may be traced in the CO-tracer field itself.

Using our own MM5- reconstruction trajectory information (3) to find an approximate plume starting point, we will follow our tracer simulation forward in time. Figure 2 shows a set of maps of simulated tracer CO for the 4 km and 7.5 km altitude regions. (These trace the history of material from the South Atlantic - Southern Africa source region to the observational point near the dateline. The top figure, Figure 2a, shows the situation of 12 September, 12 days before the DC-8 intercepted the plume near the 180 line. The 7.5 km map (and a 4 km map, not shown) show a large region of polluted air, in excess of 120 ppb, is sweeping out from the South African Coast, south of Madagascar at 30 E, 35 S. The MM5 back-trajectories over Africa become complex. The maps of 46igure A2a, and similar analyses of previous days sow accumulation of pollutants in the Central African region and a round-the-coast transport process.

Modeling papers (Chatfield and Delany, 1990, Garstang et al, 1996, Chatfield et al., 1996, Jenkins et al.,

1997, Chatfield et al., 1998) have described these accumulation patterns: in Africa, the continental accumulation over bring accumulating pollutants fromsouthern, eastern equatorial, and eastern Central Africa into a convergence- divergence region near the western equatorial coast. Continental accumulation and convergence-divergence are points (a) and (b) of our suggested general pattern. This process feeds a Great African Plume, which may in many cases feed CO and pollutants into a large accumulation region south of the Equator in the Atlantic Ocean.

Alternatively, approaching South Atlantic storm patterns may divert pollutants around the Cape of Good Hope toward the Indian Ocean. Two related circulation patterns, one acting both below 5 km (due to boundary layer or non-precipitating convection) and one above 5 km (typically due to venting by tropical convective clouds) seem to be operating in the complex weather leading up to the large plume shown in A2a.. In two of the trajectories shown in Figure 3, air has also passed over tropical South America. The intricacy (and, hence, uncertainty!) of the trajectories suggests that the effect of South America is part of a complex intercontinental accumulation pattern. This illustrates our observation, based on the entire two-months simulation of these general patterns: (c) a tendency toward intercontinental accumulation in the South Atlantic and (d) often, a final injection of highly polluted material as air crossed Southern Africa, with output between 9 and 15 km.

Following our air mass from Figure 2a, to 2b two days later, the 14th , the CO-rich airmass has moved rapidly out to the Central Indian Ocean to about 60 E, much as the trajectories show. Figure 2b shows a large plume migrating rapidly and directly across the Indian Ocean in a westerly jet. Figure 2c, two days later on the 16th, shows a distinct plume maximum crossing west Central Australia, its progress slowed somewhat. By the 18th, Figure 2d, the plume has reached nearly the observation longitude, approximately 170 W, just north of the north tip of New Zealand's main islands. The rapid, direct motion up to this point illustrates our general observations listed in the introduction (e) rapid and undilute, undulating transport and (f) subsidence of the plumes. The subsidence is quite episodic in this example. According to the trajectories shown, the plume then encounters a weather pattern which slows it and redirects it considerably from direct westward progress. Moving northward to 20 S and across the 180 longitude line, isentropic motion takes it downward as seen in Figure 2e (actually below the 4 km level shown). The isentropy of the analysis suggests that the plume was not affected by strong cloud or radiation effects in this looping motion, thus perhaps preserving the concentration of the plume eventually sampled. Note that at this point, CO levels above 80 ppb are still simulated. The cyclonic motion continues, and the plume rises up isentropically to the 170 E region by the 22nd (Figure 2f); finally the plume begins to be cross the dateline again to the position shown in Figure 3. The maps suggest that the simulated plume becomes largely attenuated and broadened in these final four days of complex motion. Apparently the observed plume did not disperse nearly as much. Nevertheless, the motion of the pollutant maximum plumes illustrates the general features of increasing undulation and dispersion within the Pacific Ocean atmosphere.

As we have seen, this study of progress of the pollutant plume from the South Atlantic / Southern Africa pollution source to the observation point illustrates many common features of such southern plumes. There are many variations on the plume behavior which we cannot detail, but our generalizations (a)-(g) seem to characterize many of them. Applying the similar analysis techniques to Sept.6 1997 case, we have found three more pattern: (e) a pattern of undulating but rapid undilute transport across the South Indian Ocean and Australia (f) subsidence of the plumes by both isentropic and diabatic, radiative processes (g) increasing undulation, splintering, and likelihood of dispersion as the plume moves into the Pacific Ocean, affected first by the Southern Pacific Convergence Zone and then by the Andes. Wisps of plumes probably continue to circulate around the globe.

4. CONCLUSIONS

We have illustrated a mechanism that conducts air pollution to the South Pacific from sources predominantly in Central Africa and South America. This we have called the Southern Global Plume. A frequently occurring sequence of events elaborated in the introduction has been illustrated with two case studies. We are unable to discuss our entire simulation or each plume sampled in the PEM Tropics A experiment. Our general impression is similar to the case studies, with some variation noted below. We find (a) a pattern of continental accumulation, (b) characteristic convergence and divergence associated with each continent associated with cumulonimbus convection, (c) a tendency toward intercontinental and plume merging near the source region, with (d) often a final pollutant injection by cloud convection over Southern Africa. Quite frequently, there is (e) a pattern of undulating but rapid undilute transport across the South Indian Ocean and Australia, (f) subsidence of the plumes by both isentropic and diabatic, radiative processes, especially below 9 km. Finally, there is (g) increasing undulation, splintering, and likelihood of dispersion in the Pacific. We found in our simulation also isolated incidences of two other pollution

patterns. Some low-lying plumes below 4 km seemed to trace back to nearby Australia. Additionally, there were instances in which plumes from Southeast Asia would drift westward across the Indian Ocean, perhaps reaching Africa. They would then recurve and join the general pollutant flow. Broad et al. (1998) describe this source region more fully, and find instances of trajectories recurving as far east as the region south of the Bay of Bengal. Though the illustrated trajectories do not show this, our trajectories tend to have more daily alteration in course than do the Broad et al. trajectories, since they are based on assimilated hourly wind data.

We can make some tentative suggestions about the simulation of the Southern Global Plume. We suspect that the weak variation of CO-tracer in our model was due to several causes that may be improved in more complex models. First, we expect that the grid resolution over the source regions of Africa and South America was too coarse. Vented pollution never made as concentrated plumes as should occur naturally. This would explain some differences of these results and those of Chatfield et al. (1998). Convective parameterizations more appropriate to the large grid resolution may also help. We expect all such parameterizations will need careful checking with tracer simulations; CO seems to provide a very good test.

Two other effects are more complex, and are connected. The conduction mechanism and the degree of subsidence experienced by the plumes seem to be governed by two major variables: the primary venting altitudes of cumulonimbus- borne material (8-10 km appears optimal) and the degree of radiative cooling that is simulated by the dynamical model. It is conceivable that the CCM-2 radiation as we employed it within MM5 did not provide sufficient radiative cooling. This could be due to our lack of feedback of the plume composition to MM5, or it could be a more general feature of the radiative cooling algorithm as we employed it. If this is the case, we venture that proper treatment of the whole vertical profile of radiative cooling as well as the profile of cumulonimbus detrainment must be carefully simulated to obtain good tracer distributions in remote regions. This imposes a high standard of accuracy on large regional and global atmospheric chemistry transport models!

Acknowledgments--This model development and analysis was supported by Jack Kaye under NASA Research Program 579-24-13-10, and a cooperative agreement between SJSU and NASA Ames, NCC-2-756. We appreciate the programming support of Robert Esswein, Long Li and Yvonne Chen, and the use of the National Aerodynamic Simulator and National Center for Atmospheric Research computers for portions of this work. Donald Blake and Nicola Blake of the University of California, Irvine provided hydrocarbon sample analysis for PEM-Tropics A, and the Edward Browell's DIAL Lidar group of NASA Langley contributed their ozone analyses.

REFERENCES

Arakawa. A., and V.R. Lamb, (1977) Computational design of the basic dynamical processes of the UCLA general circulation model, Methods in Computational Physics, Vol 17. *Academic Press*, 174-265.

Arakawa, A., and W. H. Schubert, (1974) Interaction of a cumulus cloud ensemble with the large scale environment., Part I. J. Atmos. Sci., 31, 674-701.

Broad, A.S., et al., (1998) Chemical characteristics of air from differing source regions during PEM-Tropics A, submitted to *J. Geophysical Res.*

Chatfield, R.B., and A. C. Delany, (1990) Convection links biomass burning to increased tropical ozone: However, models will tend to overpredict O_3, *J. Geophysical Res, 95,* 18473–18488.

Chatfield, R.B., J.A. Vastano, H.B. Singh, and G.W. Sachse, (1996) A generalized model of how fire emissions and chemistry produce African / oceanic plumes (O_3, CO, PAN, smoke) seen in Trace-A, *J. Geophysical Res, 101,* 24,279–24,306.

Pougatchev, N.S., G.W. Sachse, H.E. Fuelberg, C.P. Rinsland, Chatfield, V.S. Connors, N.B. Jones, J. Notholt, P.C..Novelli and H.G. Reichle, Jr., (1998) PEM-Tropicsarbon monoxide measurements in historical context, submitted toJ. *Geophysical Res,*.

Jenkins, G.S., K. Mohr, V.R. Morris, and O. Arino, (1997) The.role of convective processes over the Zaire-Congo Basin to the southern hemisphere ozone maximum,, *J. Geophys. Res, 102,* 18,963–18,980,.

Dickerson, R. R., et al., (1987) Thunderstorms, an important mechanism in the transport of air pollutants, *Science*,95, 460-465,.

Garstang, , M., P.D. Tyson, R. Swap, M. Edwards, P Kallberg, and J.A. Lindsay (1996) Horizontal and vertical transport of air over southern Africa, *J. Geophysical Res, 101,* 23,721–23,736.

Grell, G. A., (1993) Prognostic evaluation of assumptions usedby cumulus parameterizations. *Mon. Weather Rev.*, 121, 764-787,.

Grell, G., J. Dudhia, and D. Stauffer, (1995) A description of the fifth-generation Penn State/NCAR Mesoscale Model (MM5) NCAR/TN-398+STR, available from Milli Butterworth (butterwo@ncar.ucar.edu) of UCAR Information Support Services, $10.

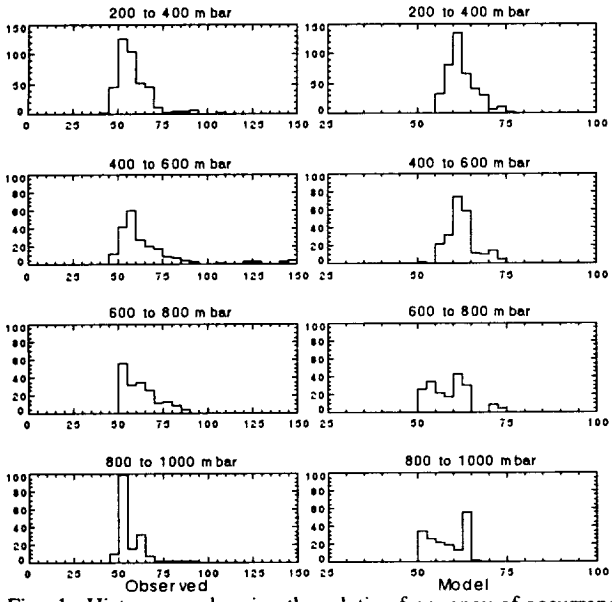

Fig. 1. Histograms showing the relative frequency of occurrence of carbon monoxide in the South Pacific. Histograms are shown for four altitude layers, each essentially representing one quarter of the tropospheric mass below 12 km. The sampling area is indicated, from 155 E near New Zealand to 100 W, including Easter Island. (a) CO, ppb, sampled along the DC-8 flight tracks made in the area, as measured by the Sachse DACOM (Differential Absorption of Carbon Monoxide) instrument on board. (b) CO tracer from our model, as sampled along the same DC-8 flight track. Note different scale.

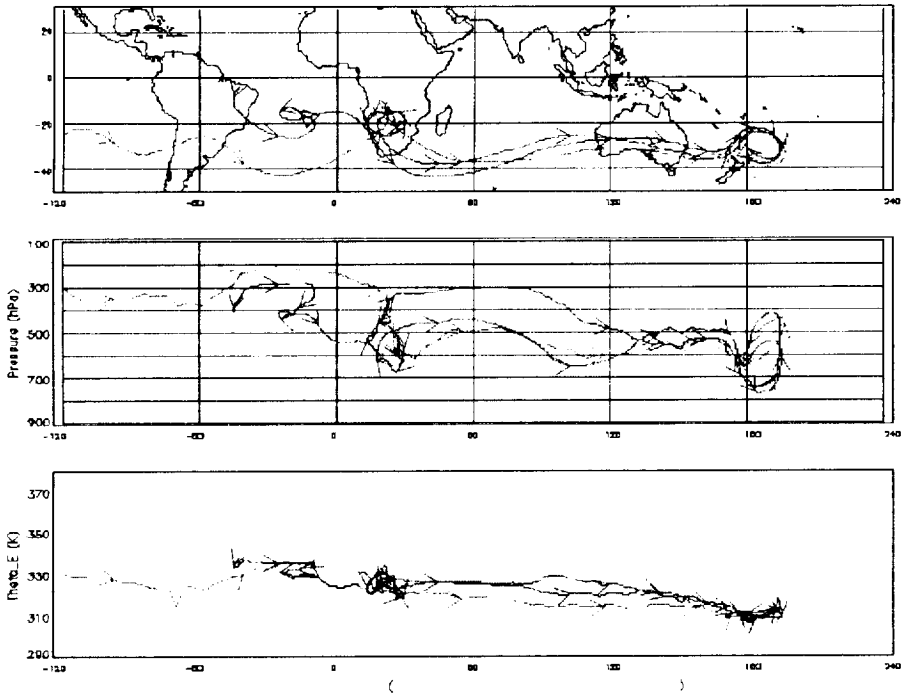

Fig. 3. Back trajectories from several points along and near the region of DC-8 decent of September 23-24, 1996. Top panel maps trace back to source regions over southern Central Africa and Brazil. Middle panel shows altitude in pressure units (hPa). Arrows are plotted showing instantaneous direction every 2 days backward from the final sampling point, e.g, at Sept. 6, Sept. 4, Sept 2., etc. In (a) and (b), regions of trajectory looping and hesitation are those most typical of a larger selection of trajectories not shown: the South Atlantic, over Central Africa, and then again in the Pacific east of New Zealand (c) Pattern of change of θ_e, equivalent potential temperature, in K. Near-conservation of θ_e, suggests that the trajectory is believable, not crossing into other air masses

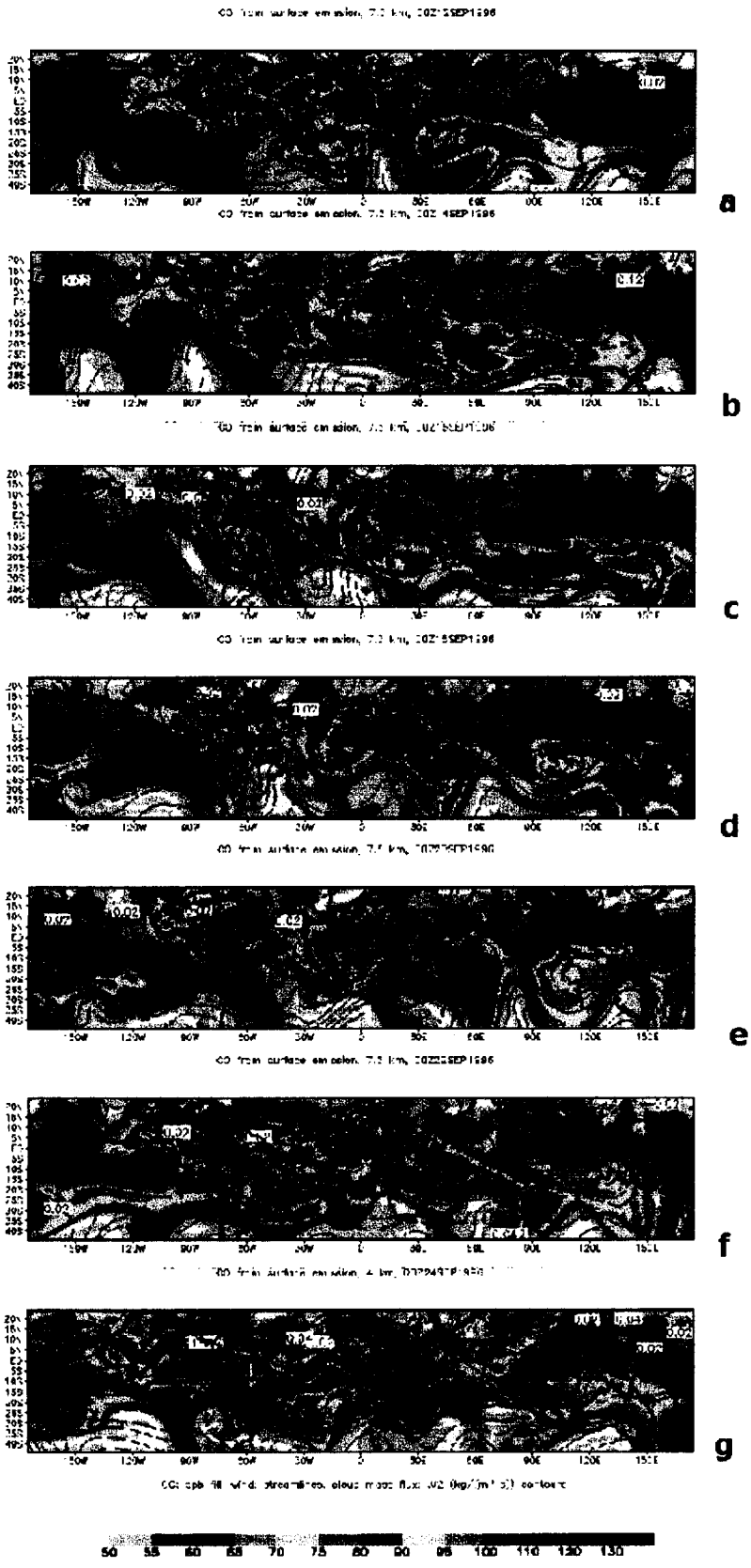

Fig. 2. Sequence of maps showing the development and propagation of the Southern Global Plume (a) Sept. 12, 00 UT, 7.5 km. (b) Sept. 14, 00 UT, 7.5 km (c) Sept. 16, 00 UT, 7.5 km, (d) Sept. 18, 00 UT, 7.5 km (e) Sept. 20, 00 UT, 4 km, , (f) Sept 22, 00 UT, 4 km. (g) The final position sampled by the DC-8 aircraft on September 24 near the 180 meridian. See text and Figure 2 to follow progress of main contributors to the plume.

APPENDIX

Meteorology of the Southern Global Plume: African and South American Fires Pollute the South Pacific

by
Zitian Guo
and
Robert B. Chatfield